



Evidence for a novel feedback loop in the Hedgehog pathway involving the seven transmembranedomain protein Smoothened and the kinase Fused.

Sandra Claret, Matthieu Sanial, Anne Plessis

► To cite this version:

Sandra Claret, Matthieu Sanial, Anne Plessis. Evidence for a novel feedback loop in the Hedgehog pathway involving the seven transmembranedomain protein Smoothened and the kinase Fused.. Current Biology - CB, 2007, Sous presse (?). hal-00162289

HAL Id: hal-00162289

<https://hal.science/hal-00162289>

Submitted on 13 Jul 2007

HAL is a multi-disciplinary open access archive for the deposit and dissemination of scientific research documents, whether they are published or not. The documents may come from teaching and research institutions in France or abroad, or from public or private research centers.

L'archive ouverte pluridisciplinaire **HAL**, est destinée au dépôt et à la diffusion de documents scientifiques de niveau recherche, publiés ou non, émanant des établissements d'enseignement et de recherche français ou étrangers, des laboratoires publics ou privés.

Evidence for a novel feedback loop in the Hedgehog pathway involving the seven transmembrane-domain protein Smoothened and the kinase Fused.

Sandra Claret ^{1,2}, Matthieu Sanial ¹ and Anne Plessis ^{1*}.

¹ Laboratoire « Génétique du Développement et Evolution », Institut Jacques Monod - Université Paris 7,

UMR 7592, CNRS/Universités Paris 6 and 7

2 Place Jussieu 75251 Paris, France

² Current address: Laboratoire « Morphogenèse et polarité », Institut Jacques Monod - Université Paris 7,

UMR 7592, CNRS/Universités Paris 6 and 7

2 Place Jussieu 75251 Paris, France

UMR 7592, CNRS/Universités Paris 6 and 7

2 Place Jussieu 75251 Paris, France

* To whom correspondence should be addressed.

E-mail: plessis@ijm.jussieu.fr

Phone: 33 1 44 27 76 08

Fax: 33 1 44 27 52 65

Short title: Fused-Smoothened regulation.

Key words: Hedgehog, Smoothened, Fused, signalling, traffic, imaginal disc, feedback loop,

Drosophila.

SUMMARY

Hedgehog (HH) is a major secreted morphogen involved in development, stem cell maintenance and oncogenesis [1, 2]. In *Drosophila* wing imaginal discs, HH produced in the posterior compartment diffuses into the anterior compartment to control target gene transcription via the transcription factor Cubitus interruptus (CI). The first steps in reception and transduction of the HH signal are mediated by its receptor Patched (PTC) [3] and the seven-transmembrane domain protein Smoothened (SMO) [4, 5]. PTC and HH control SMO by regulating its stability, trafficking and phosphorylation (for review see [6]). SMO interacts directly with the Ser-Thr protein kinase Fused (FU) and the kinesin-related protein Costal2 (COS2), which interact with each other and with CI in an intracellular “Hedgehog transducing complex” [7-9].

We show here that HH induces FU targeting to the plasma membrane in a SMO-dependent fashion and that, reciprocally, FU controls SMO stability and phosphorylation. FU anchorage to the membrane is sufficient to make it a potent SMO-dependent, PTC-resistant, activator of the pathway. These findings reveal a novel positive-feedback loop in HH transduction and are consistent with a model in which FU and SMO, by mutually enhancing each other's activities, sustain high levels of signaling and render the pathway robust to PTC level fluctuations.

RESULTS

SMO promotes the relocalization of FU from vesicles to the plasma membrane in response to HH

We produced FU tagged with RFP (RFP-FU) and SMO tagged with GFP (SMO-GFP) alone or together in Clone 8 cells (CI-8) — *Drosophila* wing imaginal disc cultured cells responsive to HH. In these conditions, pairs of proteins were overproduced, so other components were probably present at much lower levels. In the absence of HH, SMO-GFP

colocalized with RFP-FU (but not with RFP-COS2) in vesicles (Figure 1G-G'', see also [9]). HH induced the accumulation of SMO-GFP at the cell surface, but had little effect on RFP-FU alone (Figure 1B, D). When both proteins were overproduced in the presence of HH, most of the RFP-FU colocalized with SMO-GFP at the plasma membrane (Figure 1H-H''). COS2 has been reported to bind the N-terminal part of the cytoplasmic tail of SMO directly, but SMO-GFP colocalized with RFP-COS2 only when HH was present (see the Supplementary Data Figure S3 of [9]).

SMO^{ΔFU}-GFP is a mutant of SMO-GFP unable to interact with FU or to colocalize with RFP-FU in the absence of HH, due to deletion of the last 59 amino acids of SMO, which include the SMO/FU interaction domain [9]. In the presence of HH, SMO^{ΔFU}-GFP accumulated at the plasma membrane (Figure 1E-F) and colocalized with RFP-COS2 in the presence of HH (Supplementary Data Figure S3 of [9]), but did not recruit RFP-FU (Figure 1J-J'').

Thus, upon HH stimulation, SMO-GFP induces the relocation of RFP-FU to the plasma membrane. This effect is directly dependent on the region of SMO-GFP that binds FU and is unlikely to involve COS2.

The production of a form of FU tethered at the plasma membrane disrupts normal *Drosophila* development and constitutively activates the HH pathway

In imaginal wing discs, FU is required to upregulate genes responsive to high levels of HH [10-12]. We investigated the consequences of FU relocation to the membrane, by producing a fusion between the N-terminal end of CFP-FU and GAP43 (GAP-CFP-FU) - a palmitoylated domain thought to anchor proteins in raft domains [13, 14] - in wing imaginal discs. As wild-type FU [15], GFP-FU accumulated throughout the wing imaginal disc (Supplemental Data Figure S1) and its overproduction of had no visible effect on wing

development (Figure 2B). By contrast, GAP-CFP-FU gave a very strong wing phenotype characteristic of strong ectopic HH pathway activation (Figure 2C, D and data not shown).

In the wing disc, HH emanating from the posterior cells stabilizes full-length CI (CI-FL) [16] and induces the differential transcription of target genes in anterior cells near the antero-posterior boundary [10, 12, 17]. Consistent with its phenotypic effects, GAP-CFP-FU (but not GFP-FU) overproduction in the wing disc led to ectopic anterior (i) accumulation of CI-FL (Figure 2E and H) and (ii) expression of all the HH-responsive genes tested, including those known to respond to the highest levels of HH, including *ptc* itself, *collier (col)* and *engrailed (en)* (Figure 2F-L').

In *fu*- mutants, the production of GAP-CFP-FU rescued the (*fu*⁻) phenotype and even led to overactivation of the pathway at the antero-posterior border (Figure 2M-N and Supplemental Data Figure S2), thus excluding the possibility that GAP-CFP-FU acted by sequestering a negative regulator of the endogenous FU protein. In contrast, the overproduction of COS2 or SU(FU), two known antagonists that interact physically with FU [18, 19], strongly decreased the activating effects of GAP-CFP-FU (Supplemental Data Figure S3). Accordingly, the loss of SU(FU) function led to an aggravation of the phenotypes induced by GAP-CFP-FU. The loss of one copy of *cos2* had no effect (data not shown).

In conclusion, the overproduction of a form of FU anchored to the membrane is sufficient to induce medium- to high-level activation of the HH pathway in the wing disc, raising the possibility that the subcellular distribution of FU plays a key role in controlling its activity.

The wild-type and membrane-tethered forms of FU control the subcellular distribution, stability and phosphorylation of SMO

Surprisingly, the loss of one dose of the *smo* gene (flies heterozygous for the amorphic *smo*^{D16} allele), [4, 20] had an epistatic effect on the activating effects of GAP-CFP-FU, restoring an almost wild-type wing phenotype and normal levels of PTC accumulation (Figure 2O-O' and P-P'). This is the first report of a dominant effect of a loss-of-function allele of *smo* and argues for a dose-dependent effect of *smo*.

SMO is stabilized in response to HH in the posterior compartment and in the anterior cells close to the antero-posterior boundary [21]. In GAP-CFP-FU-producing discs (but not in GFP-FU-producing discs), SMO accumulated throughout the disc, even in the anterior region, which contains no HH (Figure 3A, B and D). We also induced clones of cells homozygous for *fu*^{Z4}, a deficiency including the *fu* gene [22]. In the posterior compartment, where high levels of HH normally stabilize SMO, *fu*^{Z4}/*fu*^{Z4} clones displayed low levels of endogenous SMO protein accumulation (Figure 3C and C'). These results suggest that FU is required in the wing imaginal disc for full SMO stabilization in cells receiving the HH signal and that, in the absence of HH, the anchorage of FU to the membrane is sufficient to increase SMO accumulation.

In CI-8 cells without HH, GAP-CFP-FU (alone or with SMO-RFP) was present at the plasma membrane and in large vesicular structures beneath the plasma membrane (Figure 1K-K'' and data not shown). In cotransfected cells, SMO-RFP, which is normally vesicular in the absence of HH, was present at the plasma membrane where it almost completely colocalized with GAP-CFP-FU (Figure 1K-K''). In contrast, the distribution of SMO^{ΔFU}-RFP was not affected by GAP-CFP-FU (Figure 1L-L''), indicating that GAP-CFP-FU recruited SMO-RFP by interacting with it. In similar conditions (without HH), RFP-COS did not colocalize with SMO-GFP (Supplementary Data Figure S3 in [9]), and GAP-CFP-COS2 neither interacted with SMO-RFP nor relocalized it, despite being present at the plasma membrane

(Supplemental Data Figure S4). Both these data argue against a potential bridging effect of endogenous COS2.

In conclusion, (i) the constitutive activation of the HH pathway induced by GAP-CFP-FU expression requires endogenous SMO, (ii) GAP-CFP-FU can recruit SMO (but not SMO^{ΔFU}-RFP) to the membrane of C1-8 cells (iii) GAP-CFP-FU and FU stabilize SMO *in vivo*. Thus, FU acts, directly or indirectly, on SMO.

The activating effects of FU anchored to the membrane cannot be inhibited by *ptc* overexpression

PTC has a negative effect on SMO and its overproduction inhibits the HH pathway [21, 23] (Figure 2Q). However, PTC overproduction was unable to attenuate the effects of GAP-CFP-FU (Figure 2 R). In contrast, PTC overproduction was able to counter the activating effects of GFP-SMO-GAP or SMO^{ΔFU}, which activate the HH pathway at low and high levels, respectively (Supplemental Data Figure S5).

When *ptc* was expressed alone with the *MS1096* driver, which gives strong expression in the dorsal compartment of the wing pouch [24] (Supplemental Data Figure S6), much lower levels of posterior SMO accumulation were observed in the dorsal compartment (Figure 3E). Coexpression of the GAP-CFP-FU construct, but not of GFP-FU, (Figure 3F and G) abolished this effect of PTC, as it resulted in uniform SMO accumulation. This result is consistent with a previous report [25] showing that the increase in SMO accumulation in response to HH observed when PTC levels are reduced (by RNA interference) is abolished by a decrease in FU levels.

Thus, our data demonstrate that the activation and stabilization of SMO by GAP-CFP-FU cannot be downregulated by PTC.

Wild-type FU and FU anchored to the membrane modulate the phosphorylation of SU(FU) and SMO

FU is required for the phosphorylation of SU(FU) [25]. We investigated the effects of GAP-CFP-FU on SU(FU) phosphorylation, by western blot analysis of imaginal wing disc extracts (Figure 3H). In wild-type discs and in discs expressing GFP-FU, a small fraction of SU(FU) was phosphorylated, probably due to the presence of endogenous HH. The phosphorylated SU(FU) fraction was more abundant in discs producing GAP-CFP-FU (driven with *MS1096*). Thus, anchoring FU to the membrane can promote the phosphorylation of SU(FU).

SMO is hyperphosphorylated in response to HH. This phosphorylation involves the cAMP-dependent protein kinase (PKA) and casein kinase I (CKI) and is necessary for the activation of SMO [26-28]. We monitored the phosphorylation of SMO tagged with HA (SMO-HA) in extracts of *Drosophila* S2 cells (Figure 3I). In the absence of HH, GFP-FU led to the appearance of slowly migrating forms of SMO-HA (green arrowhead), at intermediate positions between the unphosphorylated form of SMO-HA (black arrowhead) and the hyperphosphorylated forms induced by HH (red arrowhead). These intermediate forms corresponded to phosphorylated isoforms of SMO-HA, as they disappeared after incubation of the extracts with alkaline phosphatase (Figure 3J). GAP-CFP-FU had a similar effect on SMO-HA phosphorylation (Figure 3I). GAP-CFP-FU also reproducibly stabilized SMO-HA (see Figure 3 and for supplemental controls the Supplemental Data Figure S7), resulting in larger amounts of phosphorylated SMO-HA than obtained with GFP-FU.

Thus, both GFP-FU and GAP-CFP-FU can induce the phosphorylation of SMO, and our data suggest that FU may activate the pathway by increasing the amount of phosphorylated SMO accumulated.

The kinase activity of FU is involved both in the phosphorylation of SMO and the activating effects of GAP-CFP-FU

We investigated whether the phosphorylation of SMO-HA induced by FU was dependent on the kinase activity of FU, by testing two mutants of FU (Figure 2A): GFP-FU-DANA, mutated for two amino acids crucial for the phospho-transfer reaction, and GFP-FU-AS, in which a conserved residue (Thr 158) potentially involved in activating the auto-phosphorylation of FU was modified. Both mutants were shown to have lost their ability to enhance the transcriptional response of an HH-sensitive reporter gene in S2 cells [29]. We found that GFP-FU-DANA induced no phosphorylation of SMO-HA (Figure 3I), whereas FU-AS induced only very low levels of phosphorylation (data not shown). Similar results were obtained with GAP-CFP-FU-DANA (Figure 3K) and GAP-CFP-FU-AS (data not shown). However, these two proteins were present at the plasma membrane, where they recruited SMO-RFP (Supplemental Data Figure S8). Thus, neither its kinase activity nor its Thr 158 are required for the interaction of GAP-CFP-FU with SMO or the recruitment of SMO at the plasma membrane but they are required to promote SMO phosphorylation.

FU-GFP-DANA expression unexpectedly induced a [*fu*⁻]-like phenotype and FU-GFP-AS induced mild downregulation of the HH pathway (Supplemental Data Figure S8). GAP-CFP-FU-AS and GAP-CFP-FU-DANA gave similar phenotypes, indicating that the negative effects of FU-DANA/AS could not be overcome by tethering these molecules to the membrane. As these mutants of CFP-FU, (with or without their GAP anchor) recruit FU-GFP to the plasma membrane (Supplemental Data Figure S9), they may exert their dominant negative effects by dimerizing with endogenous FU.

We detected no effect of GFP-FU or GAP-CFP-FU on the phosphorylation of SMO-HA induced by HH. Nevertheless, GAP-CFP-FU-DANA (and to a lesser extent, GFP-FU-DANA)

significantly decreased the fraction of SMO-HA phosphorylated in response to HH (Figure 3K and data not shown). Moreover, SMO^{ΔFU}-GFP, which cannot interact with FU, displayed a lower fraction of phosphorylated isoforms in response to HH than SMO (Figure 3L and Supplemental Data Figure S10). Thus, both the kinase activity of FU and the interaction between FU and SMO are required for full SMO phosphorylation in response to HH.

DISCUSSION

This work provides new information about (i) the mechanisms by which the activation of SMO is transduced to its cytoplasmic effector FU, (ii) the mechanisms of FU activation, and (iii) a novel positive feedback loop between FU and SMO.

Here and in a previous study [9], we provide evidence that SMO controls the subcellular distribution of two of its physical partners, FU and COS2, recruiting them to the plasma membrane in response to HH. Our data also suggest that FU may link COS2 to SMO in a vesicle-associated complex in the absence of HH, whereas FU and COS2 may independently bind SMO at the plasma membrane in the presence of HH. Thus, HH may not only promote, via SMO, the recruitment of FU and COS2 to the plasma membrane, it may also modulate the nature of interactions between these three proteins.

Several non exclusive mechanisms seem to be involved in controlling FU activity. First, the forced localisation of FU at the membrane induces strong SMO-dependent activation of the pathway in the wing. This study is the first to report a dominant active form of this type of kinase. Second, we show here that the presence of a conserved Thr in the activating loop is important for the promotion of full SMO phosphorylation and for the activating effects of GAP-FU. Thus, as FU is known to be phosphorylated in response to HH [30], the phosphorylation of this loop — by auto-phosphorylation or by other kinases — may be a key

element in FU regulation. Third, HH may regulate FU by controlling its dimerization or its interaction with potential regulatory proteins. Possible FU dimerization is consistent with (i) the reported interaction between the regulatory domain of FU and its kinase domain [31], (ii) the recruitment to the plasma membrane of wild-type FU by the wild-type and mutant forms of GAP-FU (Supplemental Data, Figure S8), and (iii) the dominant negative effects of FU mutants with modified kinase domains (see Supplemental Data Figure S2 and 8).

We present here evidence for of a novel, positive feedback loop in which SMO and FU enhance each other's activities. Indeed, SMO promotes the relocalization of FU to the plasma membrane and is required for the activating effects of GAP-FU, whereas both GAP-FU and FU control SMO stability and phosphorylation. FU kinase activity is required for SMO phosphorylation and for the activating effects of GAP-FU, but not for its association with SMO. FU may phosphorylate SMO directly or may act on other substrates, indirectly facilitating SMO phosphorylation, inhibiting phosphatases or stabilizing phosphorylated SMO. Both FU activity and its interaction with SMO seem to be required for full hyperphosphorylation of SMO in response to HH.

In the wing disc, FU is required principally for responses to the highest levels of HH present at the antero-posterior border [10-12], where SMO is active despite the strong upregulation of *ptc*. The effects of GAP-FU and FU on SMO reported here provide the first clues to a putative mechanism (FU-dependent phosphorylation and stabilization of SMO), potentially accounting for the resistance of SMO to the high level of PTC induced by HH in responding cells.

We propose the following model: (i) The HH-induced relocalization of SMO to the plasma membrane leads to the recruitment of FU and COS2 at this membrane. (ii) FU, in turn, acts on SMO, probably by further enhancing its phosphorylation, to stabilize it further and prevent its inhibition by PTC. It is not yet possible to determine whether FU regulates SMO directly or

indirectly. The kinesin COS2 may be also part of this regulatory loop. (iii) The stabilized, activated SMO/FU/COS2 complex at the plasma membrane then promotes the accumulation and activation of CI-FL, leading to the activation of HH target genes, including *ptc*.

We previously reported that SMO^{ΔFU}, which does not bind FU, is constitutively active, suggesting that FU may also act as a negative regulator of SMO in the absence of the HH signal [9]. Thus, FU may act as a switch, sensing the level of HH, inhibiting SMO in the absence of HH or activating the pathway in response to high levels of HH. Interestingly, the existence of such regulatory loops may account for the bistability properties of signaling pathways and explain how graded levels of signal may act as morphogens, leading to differential cell responses (for review see [32]).

In conclusion, we found that FU was recruited by SMO at the plasma membrane in response to HH and that this recruitment was directly dependent on the physical interaction of FU with SMO. We also found that the expression of a membrane-anchored form of FU (GAP-FU) constitutively activated the HH pathway, indicating that FU activity may be regulated by its subcellular location. Surprisingly, the activating effects of GAP-FU require a wild-type dose of endogenous SMO. We also report evidence that (i) FU and GAP-FU induce the phosphorylation of SMO, (ii) GAP-FU recruits SMO to the plasma membrane, (iii) GAP-FU renders SMO resistant to the destabilizing effects of PTC and (iv) FU controls the level of accumulation of SMO in the wing imaginal disc. Thus, our data demonstrate that FU, which is generally considered to be an effector of SMO, can also act on SMO.

EXPERIMENTAL PROCEDURES

Plasmids

All expression vectors were constructed by the Gateway recombination method (Invitrogen). The constructs used here are presented in the supplemental data.

Cell culture and transfection

Cl-8 cells were cultured as previously described [33]. Cells were plated on concanavalin A-coated coverslips and incubated for 24 h. Transient transfections were then carried out using FlyFectin (OZ bioscience). S2 cells were cultured in Schneider medium and transfected using Effectene reagent (Qiagen). Before observation, cells were fixed by incubation for 30 minutes with 4% paraformaldehyde.

Imaginal disc immunostaining and imaging (see also supplemental data).

The primary antibodies used were: mouse anti-PTC, 1/100 [24], mouse anti-EN, 1/1000 (4D9, from DSHB [34]), mouse anti-SMO, 1/1000 (20C6, from DSHB, [25]), rat anti-CI, 1/5 (2A1, [35]), rabbit anti-COL, 1/250 [11] and rabbit polyclonal anti- β -galactosidase, 1/1000 (from ICN/Cappel). Secondary antibodies were obtained from Jackson ImmunoResearch Laboratory and were all used at a dilution of 1/200.

All the images of wing imaginal discs presented were acquired with a Leica-SP2-AOBS microscope except when indicated otherwise.

Western blotting

Proteins were extracted from wing discs by the NaOH/TCA method [36] and from transfected S2 cells, using RIPA buffer. Protein extracts corresponding to 20 wing discs or to 30 μ g of S2 cells extracts were fractionated by SDS-PAGE and transferred to a nitrocellulose membrane (Schleicher & Schuell). Blots were probed with a polyclonal rabbit antibody specific for SU(FU) [19], a mouse monoclonal antibody specific for TUB (Sigma) or a rat monoclonal antibody against HA (Roche). Bound antibody was detected with secondary antibody conjugated with horseradish peroxidase (Biovalley Vector Lab.). The

immunolabeled bands were detected with the enhanced chemiluminescence detection system (Supersignal West Pico Chemiluminescent Substrate, Pierce).

ACKNOWLEDGMENTS

We thank S. Cohen, I. Guerrero, J. Jiang, L. Ruel, F. Schweisguth, P. Thérond, C. Tong, M. van den Heuvel, A-M Voie and A. Zhu for providing plasmids, antibodies, fly strains, cell lines and technical advice, S. Malpel for his participation in the construction of the GAP-CFP-FU vector and of the transgenic *UAS-GAP-CFP-fu* flies, R. Benkiran for her participation in some experiments, A. Brigui, C. Chamot, M. Coppey, R. Karess, C. Lamour-Isnard, T. Piolot, F. Schweisguth, M. Tramier and H. Tricoire for their help and support. We also thank the Cell Press editors and anonymous reviewers for their suggestions. The monoclonal antibodies obtained from the Developmental Studies Hybridoma bank were developed under the auspices of the NICHD and maintained by the University of Iowa. *Drosophila* embryo injections were carried out by BestGene Inc Service. English usage was corrected by Alex Edelman & Associates. This work was supported by the CNRS, University Paris 7 and ARC (grant no. 4797), by an ACI “Biologie du développement et physiologie integrative” (grant no. 525044). The imaging facilities were partially funded by the ARC, the region Ile de France (SESAME) and the University Paris VII. S. C. was ATER at the University Paris 7, and was also supported by “Fondation des Treilles”.

LEGENDS

Figure 1: Subcellular distribution of SMO and FU with and without HH.

Confocal images of transfected C1-8 cells expressing fluorescent tagged versions of FU and/or SMO without HH (A, C, E, G-G”, I-I”, K-K” and L-L”) or with HH (B, D, F, H-H” and J-J”).

(A-B) Transfected cells producing GFP-FU (noted FU, in red), (C-D) SMO-GFP (SMO, in green) or (E-F) SMO^{ΔFU}-GFP (SMO^{ΔFU}, in green).

(G-J) Cotransfected cells producing RFP-FU (FU, in red) with SMO-GFP (green) (-HH in G-G'' and +HH in H-H''), or SMO^{ΔFU}-GFP (SMO^{ΔFU}, in green) (-HH in G-G'' and +HH in J-J'');
 J'');

(K-L) Cotransfected cells producing GAP-CFP-FU (GAP-FU, in green) with SMO-RFP (SMO, in red) (K-K'') or SMO^{ΔFU}-RFP (red) (L-L'') in the absence of HH.

Merged pictures are shown in G''-L''. Arrow in G'': vesicular structures. Arrowhead in H'': plasma membrane.

Figure 2: Activation of the HH pathway by a form of FU anchored at the plasma membrane.

(A) Schematic representation of the FU constructs used in this study. FU kinase domain (Kin, aa 1-255, in pale gray), FU regulatory domain (Reg, aa 256-805, in dark gray). FU-DANA has two point mutations affecting the phosphor-transfer reaction. In FU-AS, Thr158 is replaced by Ala (green triangle). GAP43 domain (yellow box), fluorescent protein : GFP in green or CFP in blue.

(B-D) Wing phenotypes of flies (or imago in C) overexpressing (B) *MS1096; UAS-GFP-fu* (indicated as *gfu*); (C) *MS1096; UAS-GAP-CFP-fu* (indicated as *GAP-cfu*); (D) *UAS-GAP-CFP-fu; 71B*. 71B is a weaker driver than *MS1096*, both are expressed in the wing pouch, to similar levels, in the anterior and posterior compartments (See also in the Supplemental data the experimental procedures section and the Figure S6).

A more detailed legend to this figure is also given in the Supplemental data.

(E-L) Effects of GFP-FU alone (E-G) or fused to a GAP- anchor (GAP-CFP-FU in H, I, J-L) overproduction in wing discs under control of *MS1096* (E-J) or in clones (K, L). (E, H) CI-

FL immunolabeling, (F, I) *dpp* expression, as reported by a *dpp-lacZ* construct (nuclear β -galactosidase immunostaining, in blue, with EN immunostaining to visualize the posterior compartment, in red); (G, J) PTC immunodetection. (See also supplemental legend); (K-L) anterior clones (labeled with GFP, in green) of GAP-CFP-FU-expressing cells with *en* (red immunostaining in K) and *col* (red immunostaining in L) expression. In (K), the normal anterior expression of *en* along the A/P border is indicated by (*). The effects of GAP-CFP-FU could be seen in all anterior clones, even away from the boundary, indicating that they occurred independently of HH.

(M-N) *fu^{MI}/Y; 71B* (M) and *fu^{MI}/Y; UAS-GAP-CFP-fu; 71B* (N) wings. The fusion of the longitudinal veins (LV) 3 and 4 and narrowing of the LV3-4 intervein region are characteristic of *fu* mutants. The effect on GAP-cFU varies with the *fu* allele used (see Supplemental Data, Figure S2).

(O-P) Wing phenotype (O and P) and immunodetection of PTC (O' and P') in *smo⁺/smo⁺* (O and O') or *smo^{D16}/smo⁺* (P and P') flies expressing *UAS-GAP-CFP-fu* under control of the *MS1096* driver.

(Q-R) Wings of flies overexpressing *UAS-ptc* (Q); *UAS-ptc* and *UAS-GAP-CFP-fu* (R) under *MS1096* driver; Wings in B were obtained from dissected imagos as the adults were unable to emerge.

All wing discs in this study are oriented with the anterior to the left and the dorsal part to the bottom and the wings are shown with the anterior to the top and the proximal end to the left. 1 to 4: LV1 to LV4. All pictures are confocal sections, except for (E, G, H and J), which are epifluorescence images.

Figure 3: GAP-CFP-FU and FU modulate the levels of SMO accumulation and phosphorylation

(A-D) Immunostaining of endogenous SMO (red). Wing imaginal discs expressing the GFP-FU (A) or GAP-CFP-FU (B) construct. The asterisk in B indicates the ectopic accumulation of SMO in the anterior region. Wing disc with a posterior fu^{Z4}/fu^{Z4} clone (labeled with GFP in C', green) (C). In the anterior region, the GFP-cells are fu^{Z4}/fu^{+} and the already low level of SMO would make it difficult to see any further reduction. Nuclei are shown in gray (C'). Note that only a few (8 to 10) rows of anterior cells are shown here and that in this region, HH emanating from the P cells is still present, leading to a gradual decrease in SMO accumulation. The difference between A and P cells is therefore more visible when comparing the P cells (outside the clone) with the most anterior cells.

(D) Schematic representation of a wing imaginal disc showing both the stronger accumulation of SMO (red) in the P compartment and in A near the A/P boundary (dotted line) and the pattern of *MS1096*-driven expression, which is stronger in the dorsal compartment (dark gray stripes) than in the ventral compartment (light gray stripes) [24]. A/P: antero-posterior axis; D/V: dorso-ventral axis. See also the pattern of *GFP MS1096*-driven expression in Supplemental Data, Figure S6.

(E-G) Immunostaining of endogenous SMO in wing imaginal discs expressing *UAS-ptc* (E); *UAS-ptc* and *UAS-GFP-fu* (F) or *UAS-ptc* and *UAS-GAP-CFP-fu* (G).

In this figure, the expression of all transgenes was driven by *MS1096* at 25°C.

(H) Immunodetection of endogenous SU(FU) in extracts of *MS1096* (wt), *MS1096; UAS-GFP-fu* (*gfu*) or *MS1096; UAS-GAP-CFP-fu* (*GAP-cfu*) wing imaginal discs. Tubulin (TUB). The black arrowheads indicate the different SU(FU) isoforms.

(I) Immunodetection of SMO-HA in extracts of S2 cells transiently expressing SMO-HA with GFP as a control (1-2) or along with GFP-FU (3-4) GFP-FU-DANA (5-6) or GAP-CFP-

FU (7-8) without (-) (odd-numbered lanes) or with (+) (even-numbered lanes) HH. See also Figure S7 for the transfection and loading controls.

(J) Immunodetection of SMO-HA in the extracts analyzed in lanes 2 and 3 of panel B. Samples in lanes 1 and 3 of this panel were treated with alkaline phosphatase, but not samples in lanes 2 and 4. Here, the gel was run for a longer period than in panel (B).

(K) Immunodetection of SMO-HA in extracts of S2 cells transiently expressing SMO-HA with GAP-CFP-FU (1-2) or with GAP-CFP-FU-DANA (3-4).

(L) Immunodetection of SMO-HA in extracts of S2 cells transiently expressing SMO (1-2) or SMO^{ΔFU}-HA (3-4) without (1, 3) or with (2, 4) HH. For quantification of the phosphorylation levels see Supplemental Figure S10. Note the increased levels of SMO^{ΔFU}-HA accumulation which can be correlated with its reported increased activity [9].

REFERENCES

1. Beachy, P.A., Karhadkar, S.S., and Berman, D.M. (2004). Tissue repair and stem cell renewal in carcinogenesis. *Nature* 432, 324-331.
2. Lau, J., Kawahira, H., and Hebrok, M. (2006). Hedgehog signaling in pancreas development and disease. *Cell Mol Life Sci* 63, 642-652.
3. Nakano, Y., Guerrero, I., Hidalgo, A., Taylor, A., Whittle, J.R.S., and Ingham, P.W. (1989). A protein with several possible membrane-spanning domains encoded by the *Drosophila* segment polarity gene *patched*. *Nature* 341, 508-513.
4. van den Heuvel, M., and Ingham, P.W. (1996). *smoothed* encodes a receptor-like serpentin protein required for hedgehog signalling. *Nature* 382, 547-551.
5. Alcedo, J., and Noll, M. (1997). Hedgehog and its patched-smoothed receptor complex: a novel signalling mechanism at the cell surface. *Biol Chem* 378, 583-590.
6. Hooper, J.E., and Scott, M.P. (2005). Communicating with Hedgehogs. *Nat Rev Mol Cell Biol* 6, 306-317.
7. Robbins, D.J., Nybakken, K.E., Kobayashi, R., Sisson, J.C., Bishop, J.M., and Therond, P.P. (1997). Hedgehog elicits signal transduction by means of a large complex containing the kinesin-related protein costal2. *Cell* 90, 225-234.
8. Sisson, J.C., Ho, K.S., Suyama, K., and Scott, M.P. (1997). Costal2, a novel kinesin-related protein in the Hedgehog signaling pathway. *Cell* 90, 235-245.
9. Malpel, S., Claret, S., Sanial, M., Brigui, A., Piolot, T., Daviet, L., Martin-Lannere, S., and Plessis, A. (2007). The last 59 amino acids of Smoothed cytoplasmic tail directly bind the protein kinase Fused and negatively regulate the Hedgehog pathway. *Dev Biol* 303, 121-133.

10. Sanchez-Herrero, E., Couso, J.P., Capdevila, J., and Guerrero, I. (1996). The *fu* gene discriminates between pathways to control *dpp* expression in *Drosophila* imaginal discs. *Mech Dev* 55, 159-170.
11. Crozatier, M., Glise, B., and Vincent, A. (2002). Connecting Hh, Dpp and EGF signalling in patterning of the *Drosophila* wing; the pivotal role of *collier/knot* in the AP organiser. *Development* 129, 4261-4269.
12. Alves, G., Limbourg, B.B., Tricoire, H., Brissard, Z.J., Lamour, I.C., and Busson, D. (1998). Modulation of Hedgehog target gene expression by the Fused serine-threonine kinase in wing imaginal discs. *Mech Dev* 78, 17-31.
13. Strittmatter, S.M., Igarashi, M., and Fishman, M.C. (1994). GAP-43 amino terminal peptides modulate growth cone morphology and neurite outgrowth. *J Neurosci* 14, 5503-5513.
14. Zhu, A.J., Zheng, L., Suyama, K., and Scott, M.P. (2003). Altered localization of *Drosophila* Smoothed protein activates Hedgehog signal transduction. *Genes Dev* 17, 1240-1252.
15. Ascano, M., Jr., Nybakken, K.E., Sosinski, J., Stegman, M.A., and Robbins, D.J. (2002). The carboxyl-terminal domain of the protein kinase fused can function as a dominant inhibitor of hedgehog signaling. *Mol Cell Biol* 22, 1555-1566.
16. Aza, B.P., Ramirez, W.F., Laget, M.P., Schwartz, C., and Kornberg, T.B. (1997). Proteolysis that is inhibited by hedgehog targets Cubitus interruptus protein to the nucleus and converts it to a repressor. *Cell* 89, 1043-1053.
17. Ohlmeyer, J.T., and Kalderon, D. (1998). Hedgehog stimulates maturation of Cubitus interruptus into a labile transcriptional activator. *Nature* 396, 749-753.
18. Monnier, V., Ho, K.S., Sanial, M., Scott, M.P., and Plessis, A. (2002). Hedgehog signal transduction proteins: contacts of the Fused kinase and Ci transcription factor with the kinesin-related protein Costal2. *BMC Dev Biol* 2, 4.
19. Monnier, V., Dussillol, F., Alves, G., Lamour, I.C., and Plessis, A. (1998). Suppressor of fused links fused and Cubitus interruptus on the hedgehog signalling pathway. *Curr Biol* 8, 583-586.
20. Chen, Y., and Struhl, G. (1996). Dual roles for patched in sequestering and transducing Hedgehog. *Cell* 87, 553-563.
21. Denef, N., Neubuser, D., Perez, L., and Cohen, S.M. (2000). Hedgehog induces opposite changes in turnover and subcellular localization of patched and smoothed. *Cell* 102, 521-531.
22. Preat, T., Therond, P., Lamour, I.C., Limbourg, B.B., Tricoire, H., Erk, I., Mariol, M.C., and Busson, D. (1990). A putative serine/threonine protein kinase encoded by the segment- polarity fused gene of *Drosophila*. *Nature* 347, 87-89.
23. Johnson, L.N., Noble, M.E., and Owen, D.J. (1996). Active and inactive protein kinases: structural basis for regulation. *Cell* 85, 149-158.
24. Capdevila, J., Pariente, F., Sampedro, J., Alonso, J.L., and Guerrero, I. (1994). Subcellular localization of the segment polarity protein patched suggests an interaction with the wingless reception complex in *Drosophila* embryos. *Development* 120, 987-998.
25. Lum, L., Zhang, C., Oh, S., Mann, R.K., von Kessler, D.P., Taipale, J., Weis-Garcia, F., Gong, R., Wang, B., and Beachy, P.A. (2003). Hedgehog signal transduction via Smoothed association with a cytoplasmic complex scaffolded by the atypical kinesin, Costal-2. *Mol Cell* 12, 1261-1274.
26. Apionishev, S., Katanayeva, N.M., Marks, S.A., Kalderon, D., and Tomlinson, A. (2005). *Drosophila* Smoothed phosphorylation sites essential for Hedgehog signal transduction. *Nat Cell Biol* 7, 86-92.

27. Jia, J., Tong, C., Wang, B., Luo, L., and Jiang, J. (2004). Hedgehog signalling activity of Smoothened requires phosphorylation by protein kinase A and casein kinase I. *Nature* 432, 1045-1050.
28. Zhang, C., Williams, E.H., Guo, Y., Lum, L., and Beachy, P.A. (2004). Extensive phosphorylation of Smoothened in Hedgehog pathway activation. *Proc Natl Acad Sci U S A* 101, 17900-17907.
29. Fukumoto, T., Watanabe-Fukunaga, R., Fujisawa, K., Nagata, S., and Fukunaga, R. (2001). The fused protein kinase regulates Hedgehog-stimulated transcriptional activation in *Drosophila* Schneider 2 cells. *J Biol Chem* 276, 38441-38448.
30. Therond, P.P., Knight, J.D., Kornberg, T.B., and Bishop, J.M. (1996). Phosphorylation of the fused protein kinase in response to signaling from hedgehog. *Proc Natl Acad Sci U S A* 93, 4224-4228.
31. Ascano, M., Jr., and Robbins, D.J. (2004). An intramolecular association between two domains of the protein kinase Fused is necessary for Hedgehog signaling. *Mol Cell Biol* 24, 10397-10405.
32. Lander, A.D. (2007). Morpheus unbound: reimagining the morphogen gradient. *Cell* 128, 245-256.
33. van Leeuwen, F., Samos, C.H., and Nusse, R. (1994). Biological activity of soluble wingless protein in cultured *Drosophila* imaginal disc cells. *Nature* 368, 342-344.
34. Patel, N.H., Martin-Blanco, E., Coleman, K.G., Poole, S.J., Ellis, M.C., Kornberg, T.B., and Goodman, C.S. (1989). Expression of engrailed proteins in arthropods, annelids, and chordates. *Cell* 58, 955-968.
35. Motzny, C.K., and Holmgren, R. (1995). The *Drosophila* cubitus interruptus protein and its role in the wingless and hedgehog signal transduction pathways. *Mech. Dev.* 52, 137-150.
36. Riezman, H., Hase, T., van Loon, A.P., Grivell, L.A., Suda, K., and Schatz, G. (1983). Import of proteins into mitochondria: a 70 kilodalton outer membrane protein with a large carboxy-terminal deletion is still transported to the outer membrane. *Embo J* 2, 2161-2168.

Figure 1

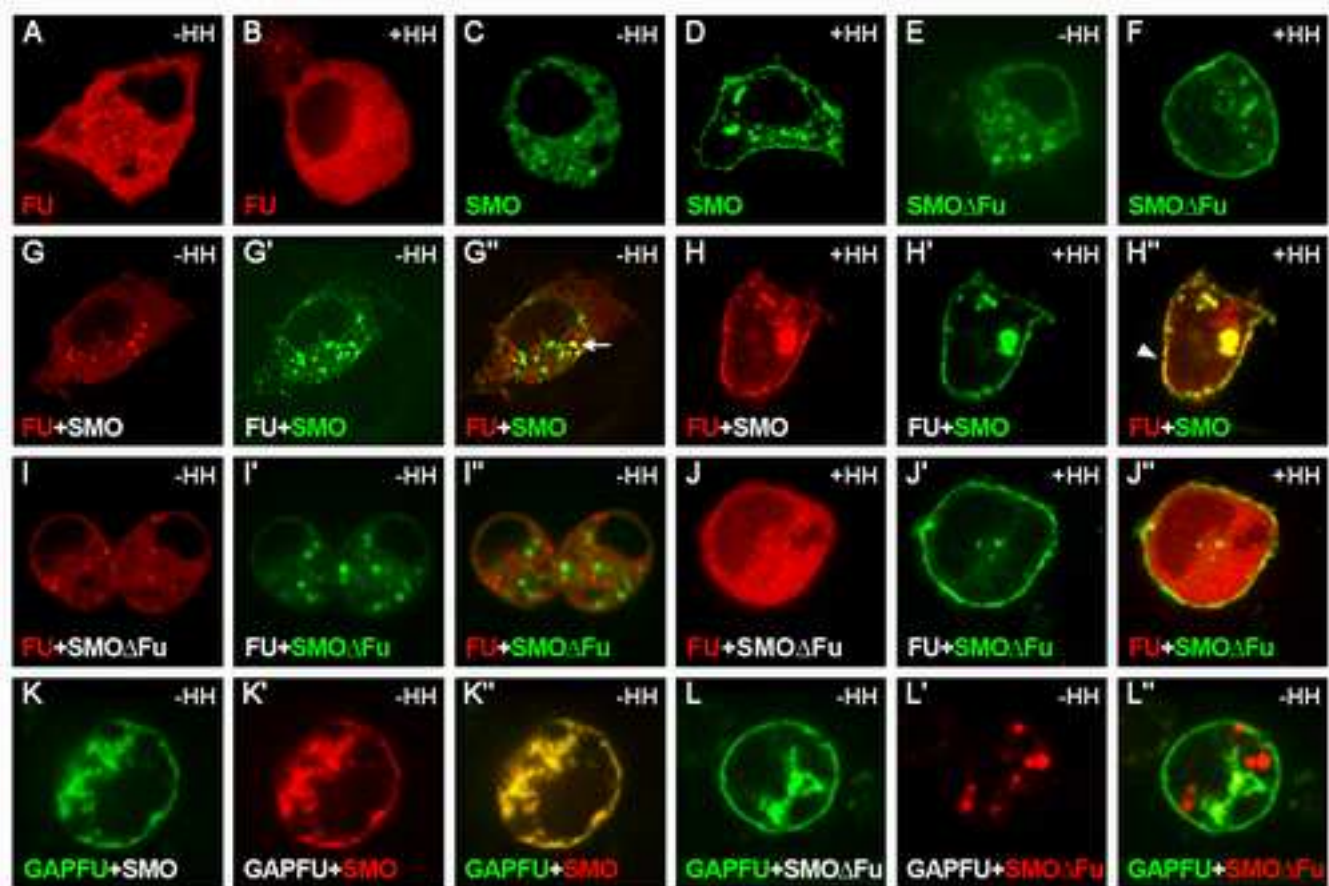


Figure 2

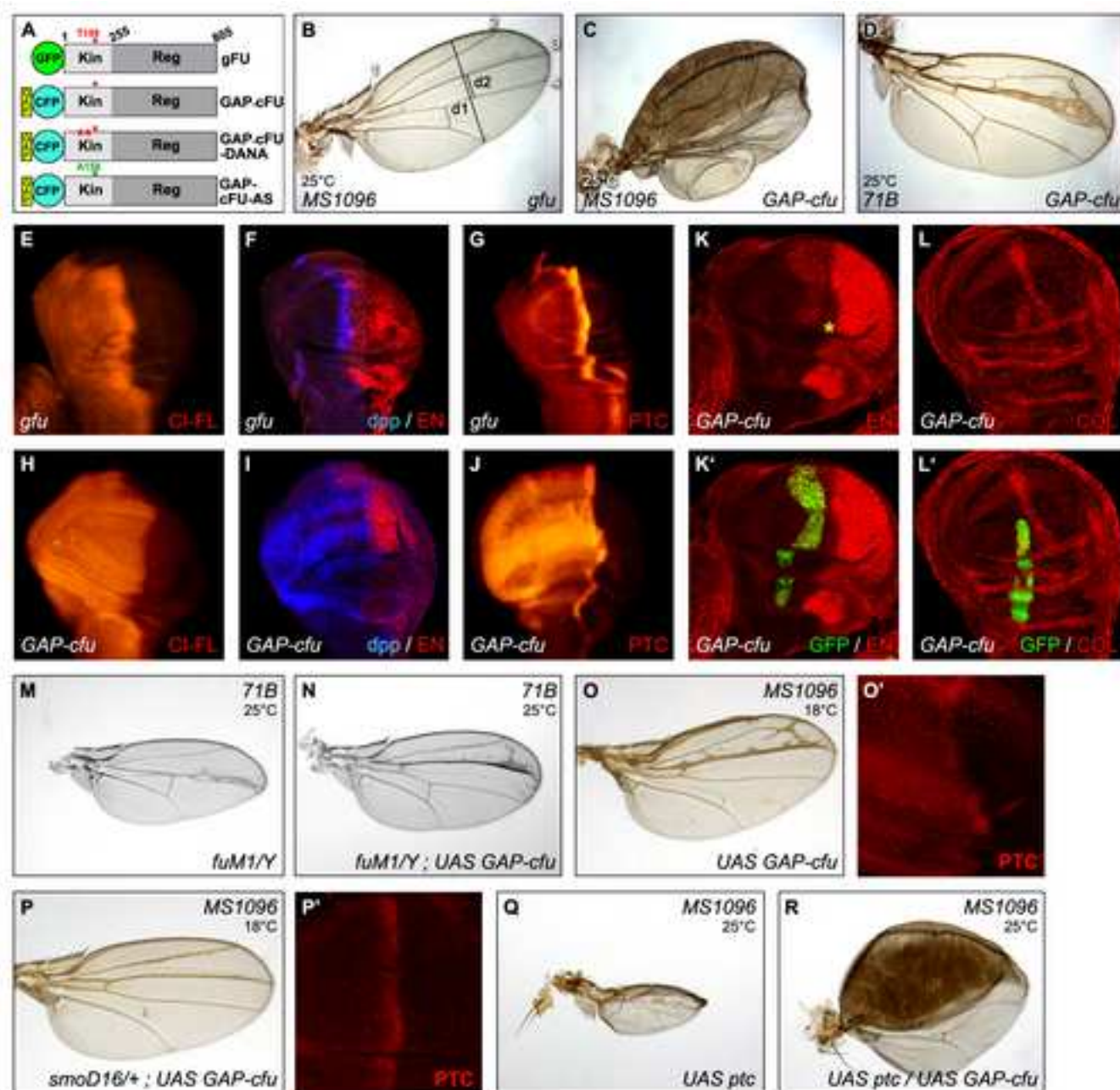
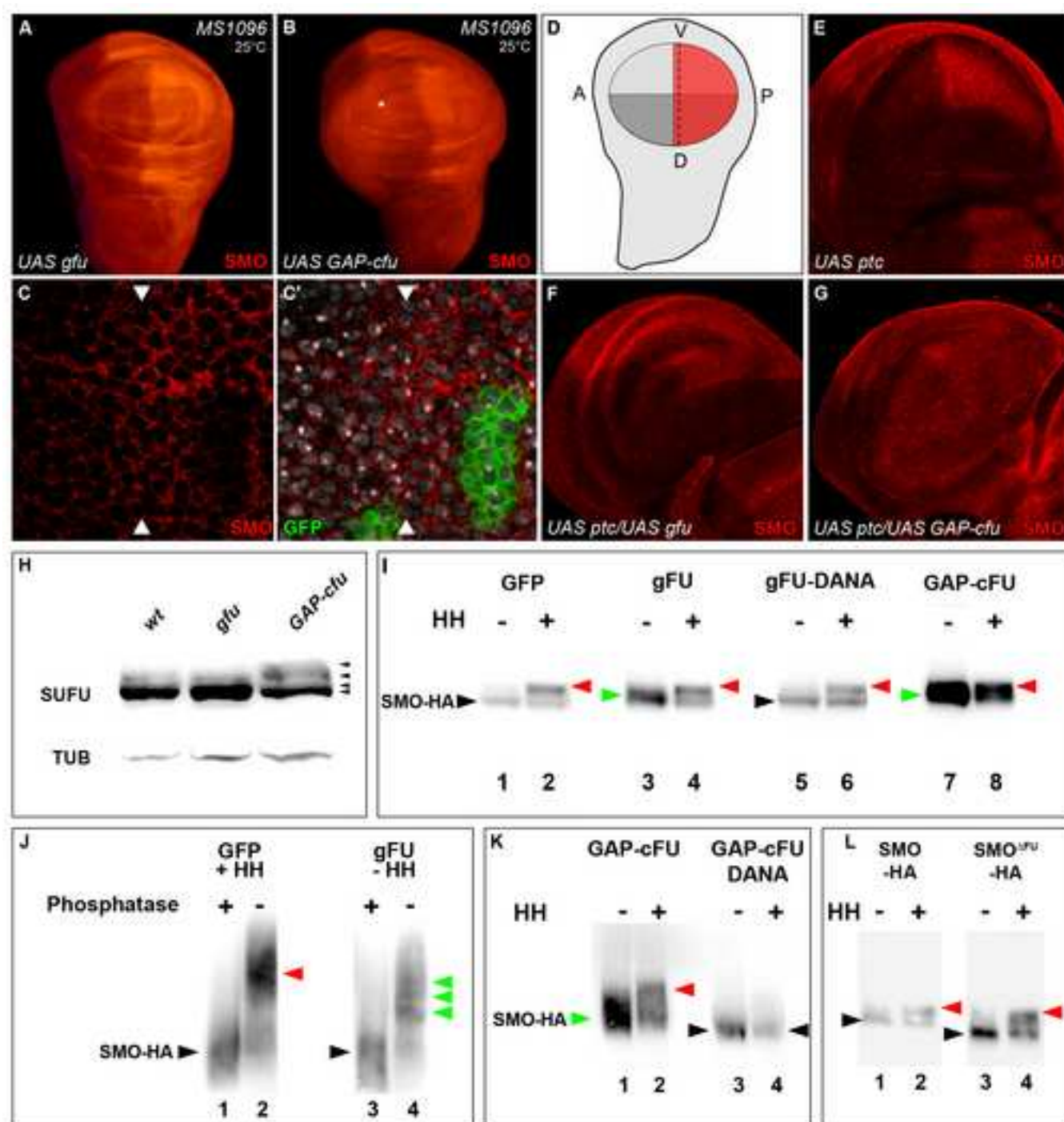


Figure 3



SUPPLEMENTAL DATA

Supplemental legends to Figure 2:

(B-D): The *MS1096; UAS-GAP-cfu* flies were unable to emerge from pupae, probably due to their enlarged and inflated wings. Imago from *MS1096; UAS-GAP-cfu* dissected pupae (C) present wings with the A compartment invaded by ectopic vein tissue associated with supernumerary campaniform sensillae, which are specific to regions controlled by high levels of HH (Figure 2C and data not shown).

d1 and *d2* are the distances measured with ImageJ software. The average ratio $d2/d1$ of flies over-expressing or not over-expressing the gFU and GAP-cFU constructs under control of the *71B* driver shows an increase in LV3/LV4 intervein tissue: $d2/d1 = 0.22 \pm 0.01$ for WT wings, 0.22 ± 0.01 for *UAS-gfu* wings and 0.25 ± 0.04 for *UAS-GAP-cfu* wings. Note that GAP-cFU had no effect on the innervated double-row bristles. (K-L): These effects were observed in all anterior clones in the wing pouch, even away from the boundary, indicating that they occurred independently of HH. These effects are only observed within the clone limits. Posterior clones have no effect (data not shown).

Supplemental Figures:

Figure S1: Accumulation and subcellular localization of GAP-CFP-FU in the wing imaginal disc

As reported for endogenous FU, overexpressed GFP-FU (A) and GAP-CFP-FU (B) are more abundant in the A compartment (where there is little or no HH) than in the P compartment. Although we cannot conclude that GAP-cFU is also destabilized by the HH signal, it does appear to be sensitive.

(C and D) are magnified views of apical and basolateral confocal sections, respectively, of a wing imaginal disc expressing GAP-cFU. (E) A Xz view reconstruction of the wing pouch across the A/P axis. GAP-FU is localized principally at the plasma membrane on the apical side of the disc, and is also present in the vesicular structure below. The expression of GFP-FU and GAP- CFP-FU was driven by *MS1096* at 25°C, a driver equally expressed in the anterior and posterior compartments (See Figure S6). The A/P axis is indicated by two arrowheads, in A to D, with A on the left. In E, the apical side is up. In (A) and (B), scale bars correspond to 50 μm , and in (C-E), scale bars correspond to 10 μm . Xz view reconstructions were obtained using ImageJ

software (Rasband, W.S., ImageJ, U. S. National Institutes of Health, Bethesda, Maryland, USA, 1997-2005).

Figure S2: Effects of *fu*⁻ mutations on the activating effects of GAP-CFP-FU

(A) Wild-type wing. (B) Wing overexpressing the GAP-CFP-FU construct, showing widening of the LV3/LV4 intervein and a thickening of LV3. *fu*^l /Y (C), *fu*^{RX2} /Y (E) and *fu*^{M1} /Y (G) wings. Overexpression of the *GAP-CFP-fu* construct in *fu*^l /Y (D), *fu*^{RX2} /Y (F) and *fu*^{M1} /Y (H). Overexpression was driven by *71B* and wings from male insects were observed.

In all cases tested, expression of the *GAP-CFP-FU* construct (driven by *71B*, [1]) in the wing pouch, rescued the *fu*⁻ phenotype. *GAP-CFP-FU* even overactivated the pathway at the antero-posterior border, as shown by the widening of the LV3/LV4 intervein region and the expansion of LV3 tissue. The effects of *GAP-CFP-FU* were not affected in the *fu*^{RX2} mutant, but they were attenuated, although not abolished in *fu*^l and *fu*^{M1} mutants. Thus, in the presence of high levels of HH (near the antero-posterior border) the activating effects of *GAP-cFU* did not require the kinase activity of endogenous FU. This indicates that the activating effects of *GAP-FU* do not simply result from the activation of endogenous FU. However, in the presence of only small amounts of HH and in the absence of HH, the activation by *GAP-CFP-FU* was reduced by the presence of an endogenous FU protein with an altered kinase domain. There are several possible explanations for this, including a dominant negative effect of endogenous FU with a mutant kinase domain.

When modeling the structure of the kinase domain of FU (data not shown), the first 80 aa of FU, which are present in *fu*^{M1}) correspond to most of its N-terminal domain, called the “small lobe”. The equivalent domain in other kinases has been shown to bind different partners. A striking example is provided by SNF1 kinase, a protein kinase closely related to FU: this kinase can form homodimers via interactions involving its small lobe [2]. The kinase domain of FU has been reported to bind to its regulatory domain [3, 4] and to its putative target SU(FU) [5]. Thus, the first 80 aa of *FU*^{M1} may be sufficient to induce a dominant-negative effect.

Figure S3: GAP-cFU-dependent activation of the HH pathway is regulated by the inhibitory regulators SU(FU) and COS2

The overexpression of various UAS transgenes was driven by *MS1096* at 25°C (A-C) or at 18°C (D-G) (as indicated). The wing overexpressing SU(FU) (A) had only a very weak phenotype, if at all (e.g. distal extra vein near LV3). The overexpression of SU(FU) almost abolished the phenotype induced by GAP-cFU overexpression (compare C with B). This decrease is not due to the dosage of GAL4 protein controlled by a second UAS (data not shown). The loss of *Su(fu)* function (in flies homozygous for the amorphic mutation, *Su(fu)^{LP}*) was associated with no visible phenotype itself (data not shown), but it exacerbated the phenotype of GAP-CFP-FU-overexpressing wings (visible at 18°C, compare E with D). The overexpression of COS2 (F) strongly inhibited the HH pathway (F) and strongly decreased the GAP-CFP-FU-dependent phenotype (compare G with D).

Su(fu)^{LP} was described in [6], *UAS-cos2* was kindly provided by M. Scott [7], and *UAS-Su(fu)* was described in [8].

Figure S4: GAP-CFP-COS2 (in green) does not colocalize with SMO-RFP (in red)

Transfected S2 cells without HH.

Figure S5: The effects of PTC overproduction are not suppressed by SMO or SMO-GAP

(A-H) Wings of flies overexpressing *UAS-ptc* (A); *UAS-ptc* and *UAS-GAP-cfu* (B); *UAS-GFP-smo-GAP* (C); *UAS-ptc* and *UAS-GFP-smo-GAP* (D); *UAS-GFP-smo* (E); *UAS-ptc* and *UAS-GFP-smo* (F); *UAS-GFP-smo^{ΔFU}* (G); *UAS-ptc* and *UAS-GFP-smo^{ΔFU}* (H). The overproduction of GFP-SMO and GFP-SMO-GAP induced low and medium levels of HH pathway activation, respectively [9, 10]. GFP-SMO-GAP had a stronger effect than GFP-SMO, but a much weaker effect than GAP-CFP-FU. Coexpression of the PTC construct with those encoding GFP-SMO-GAP or GFP-SMO led to a strong decrease in wing size and a loss of wing patterning. By contrast, coexpression of the PTC construct did not attenuate the effects of GAP-cFU. Thus, the activating effects of GAP-CFP-FU act epistatically on the inhibitory effects of PTC overproduction, whereas neither GFP-SMO-GAP nor GFP-SMO has such an effect. The lack of effect of PTC on GAP-CFP-FU-

induced activation may be due to GAP-cFU inducing a very high level of activation. We do not favor this hypothesis because PTC has been reported to inhibit SMO substoichiometrically [11] and the overproduction of PTC led to downregulation of the effects of another very strong inducer of the HH pathway, SMO^{ΔFU}.

Our data suggest that FU anchored to the plasma membrane does more to SMO than just recruiting it at the plasma membrane. The comparison between SMO-GAP and GAP-FU is validated by the fact that the same GAP moiety was used to anchor SMO and FU at the membrane, and therefore should act similarly on these two proteins. The GAP domain is known to be target for palmitoylation which is supposed to anchor proteins in raft domains. Noteworthy, HH has been found in lipid rafts in *Drosophila*, and human PTC and SMO were found in raft microdomains (Rietvel et al, J Biol Chem., 1999 and Karpen et al, J Biol Chem, 2001). Note also that several receptors of the GPCR family have been shown to be regulated by palmitoylation in response to agonists (Ross, Curr Biol, 1995, Stevens et al, J Biol Chem, 2001). However, without understanding why GFP-SMO-GAP is really activated, it is difficult to speculate.

Wings in (B and G) were obtained from dissected imagos as the adults were unable to emerge.

Figure S6: Pattern of MS1096 activity.

MS1096, UAS-GFP imaginal disc. CI immunolabelling in red, GFP in green. Orientation is as in Figure 2.

Figure S7: GFP-FU, GAP-CFP-FU and GFP-FU-DANA accumulate at comparable level.

Immunodetection of FU on the blot presented in Figure 3 I.

The effects of GAP-FU on the accumulation of SMO seen in the western blot presented in Figure 3I were seen in 5 independent experiments. In each experiments the same amount of proteins were loaded in all lanes. However, to ensure that the differences of effects between Gap-FU and FU or FU-DANA were not due to differences in transfection efficiency or in the stability of the different forms of FU, we checked the levels of accumulation of the various forms of FU.

Figure S8: Effects of GAP-CFP-FU-DANA and GAP-CFP-FU-AS on SMO-RFP subcellular distribution and wing phenotype

(A-B) Cells expressing SMO-RFP (in red, A', A'', B' and B'') with either GAP-CFP-FU-DANA (in green, A, A'') or GAP-CFP-FU-AS (in green, B, B'').

(C-F) Wings of flies overexpressing forms of FU with mutations affecting their kinase domain with or without the GAP domain (*MS1096* driver at 25°C).

Figure S9: Cotargeting of wild-type FU to the plasma membrane by GAP-FU

Transfected C18 cells coexpressing different forms (WT, DANA or AS) of GAP-cFU (in green) and rFU (in red) in the absence of HH.

(A-A'') Cells cotransfected with GAP-CFP-FU and RFP-FU; (B-B'') Cells cotransfected with GAP-CFP-FU-DANA and RFP-FU; (C-C'') Cells cotransfected with GAP-CFP-FU-AS and RFP-FU.

In these three contexts, RFP-FU is recruited to the plasma membrane by the GAP-FU forms. These data indicate that FU can interact with itself. This cotargeting of FU forms is independent of AS and DANA mutation.

Figure S10: The efficiency of SMO phosphorylation in response to HH in reduced in SMO^{AFU}.

The immunoblot presented in Figure 3L was plotted using ImageJ. With SMO the HH-dependent hyperphosphorylated isoforms are always more abundant than the non phosphorylated isoform, while with SMO^{AFU} the both isoforms are equally abundant.

Supplemental experimental procedures:

Vectors: The full coding sequences (without the termination codon) of *smo* and *fu* cDNAs were amplified by PCR, and inserted into pENTR/D-TOPO by directional TOPO cloning. The RFP-FU, SMO-GFP and SMO^{AFU}-GFP expression vectors have been described elsewhere [9]. Rescue experiments demonstrated the functionality of the rFU and SMOg fusion proteins in *Drosophila* [9]. AS and DANA FU mutants were amplified by PCR from pDA-Flag-fu-AS or pDA-Flag-fu-DANA [12]. The DANA mutant has two alanine residues replacing Asp-125 and Asn-130, both of which are invariantly conserved among members of the protein kinase family and are involved in the phospho-transfer reaction. The AS mutant has an alanine residue

replacing the conserved Thr-158. The destination vectors pAWR (pAct5C-GW-mRFP) (where GW is the recombination cassette) were obtained from T. Murphy. The pUAST-nterm-m6GFP and pUAST-CFP-GW vectors were a gift from A. Brand. A sequence encoding the GAP peptide (MLCCMRRTKQVEKNDEDEDQKI) was inserted in frame with the CFP into the *Bgl*II site located just upstream from the CFP in pUAST-CFP-GW. The HH expression vector, pDA-FL Hh, was a gift from D.J. Robbins. All cloning steps were performed according to the manufacturer's instructions (Invitrogen).

Fly strains and genetics

Flies were raised at 25°C unless otherwise specified. Mutants and transgenic strains are described in the Supplemental data. Transgenic, *UAS-GFP-fu* and *UAS-GAP-CFP-fu* strains, with or without DANA and AS mutations, were obtained by a standard P-element-mediated procedure. For clonal overexpression, *hsp-flp; +/+; tub1>CD2>GAL4*, *UAS-GFP/UAS-GFP-fu* or *pUAS-GAP-CFP-fu* first instar larvae were subjected to heat shock for one hour at 38°C. Mosaic analysis with a repressible cell marker (MARCM) [13]) was carried out in larvae from crosses between *FRT19A*, *Tub-Gal80*, *hsp-flp; UAS-LacZ*, *UAS-CD8-GFP; TubGal4/TM6b* females (a gift from S. Bray) and *FRT19A fuZ4/Y* males.

MS1096 (chr. X, [14]), *71B* (chr. III, [15]), *hsp-flp; +/+; tub1>CD2>GAL4*, *UAS-GFP /TM3* [16]. *fu^l*, *fu^{MI}* and *fu^{RX2}* were described by [17]. *UAS-ptc/CyO* and *UAS-GFP-smoGAP/TM3* flies were provided by M. Scott; the *smo^{D16}* allele was provided by Van den Heuvel and is thought to be a probable null allele [18].

Analysis of wings

Wings were dissected in 70% ethanol, mounted in Hoyers medium and examined for their vein and wing margin bristle phenotypes. Using ImageJ software, we measured both the width of the LV3-LV4 intervein (d1) and that of the entire wing (d2), and then calculated the d1/d2 ratio. At least 30 adults were examined in each experiment.

Imaginal disc immunostaining

Imaginal discs from third instar wandering larvae were dissected in PBS, fixed by incubation for 30 min at room temperature (RT) in 4% paraformaldehyde, washed and permeabilized by three incubations for 10 minutes each in PBS + 0.1% Tween (PBST). They were blocked by incubation for one hour in PBST + 2% BSA, then overnight at 4°C with the primary antibody. They were washed three times, for 10 minutes each with PBST, blocked by incubation for 1 hour in PBST + 2% BSA and incubated for 3 hours at RT with the secondary antibody (in PBST + 2% BSA). Finally, they were rinsed three times, for 10 minutes each, in PBST and mounted in Citifluor.

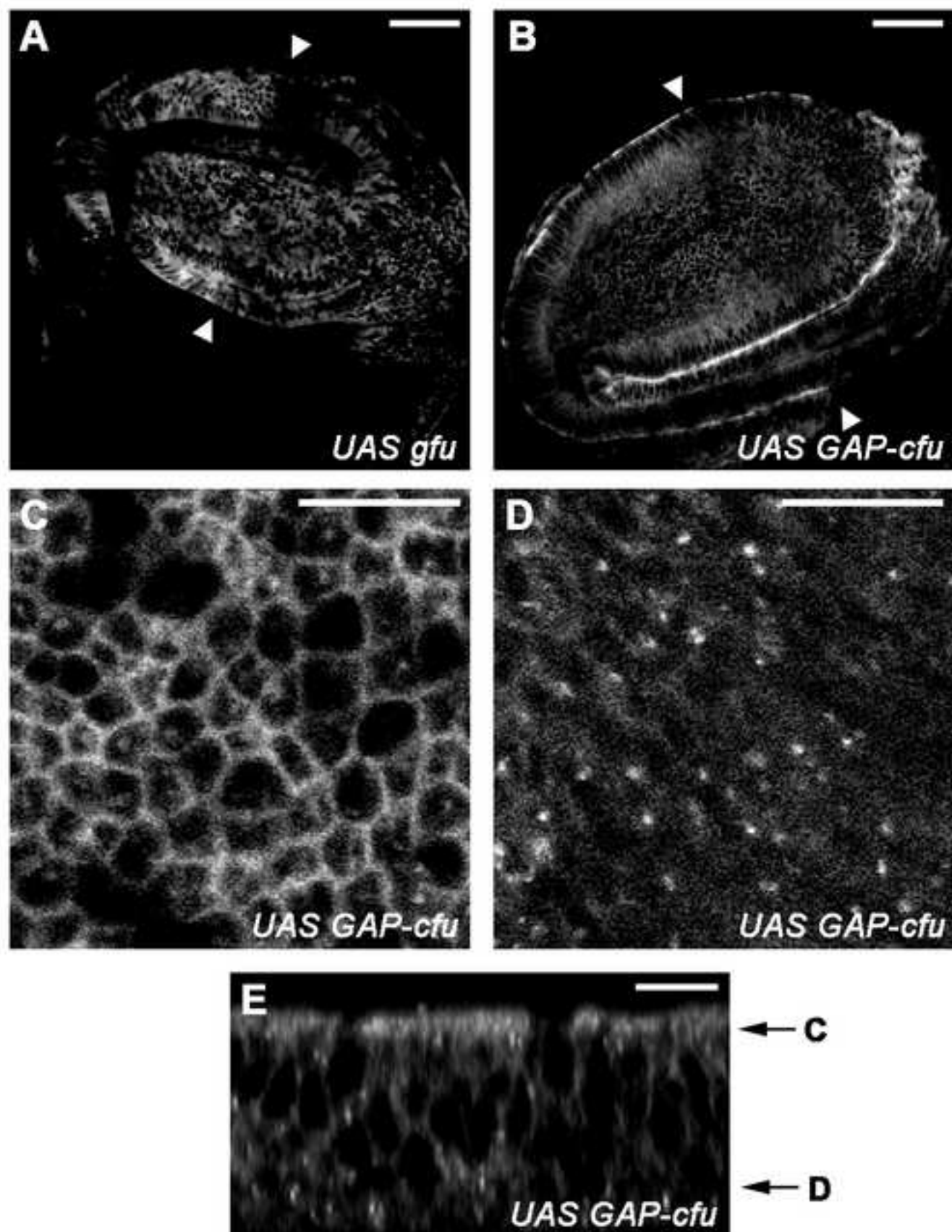
Confocal imaging

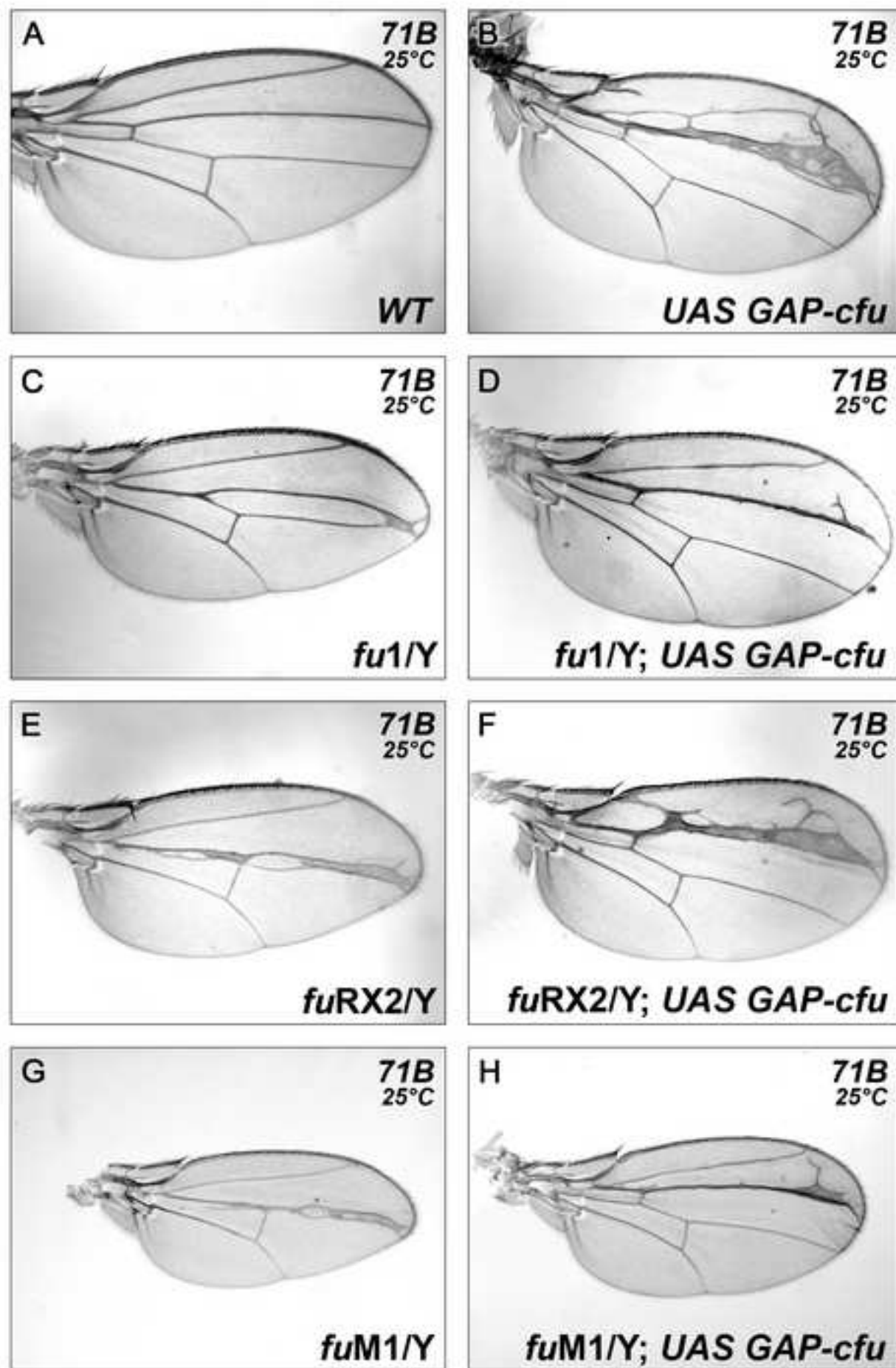
Cell culture images were acquired with a Yokogawa spinning disk confocal head coupled to a Leica inverted microscope (Leica, DMIRB). Excitation was achieved with an Argon-Krypton 75 mw laser (Melles Griot). Images were acquired with a CoolSnap HQ camera (Princeton Instruments). The whole set-up was driven by Metamorph 6.3 (Universal Imaging). The integration and wavelength switch module was designed by the firm “Errol” and the Institut Jacques Monod imaging facility.

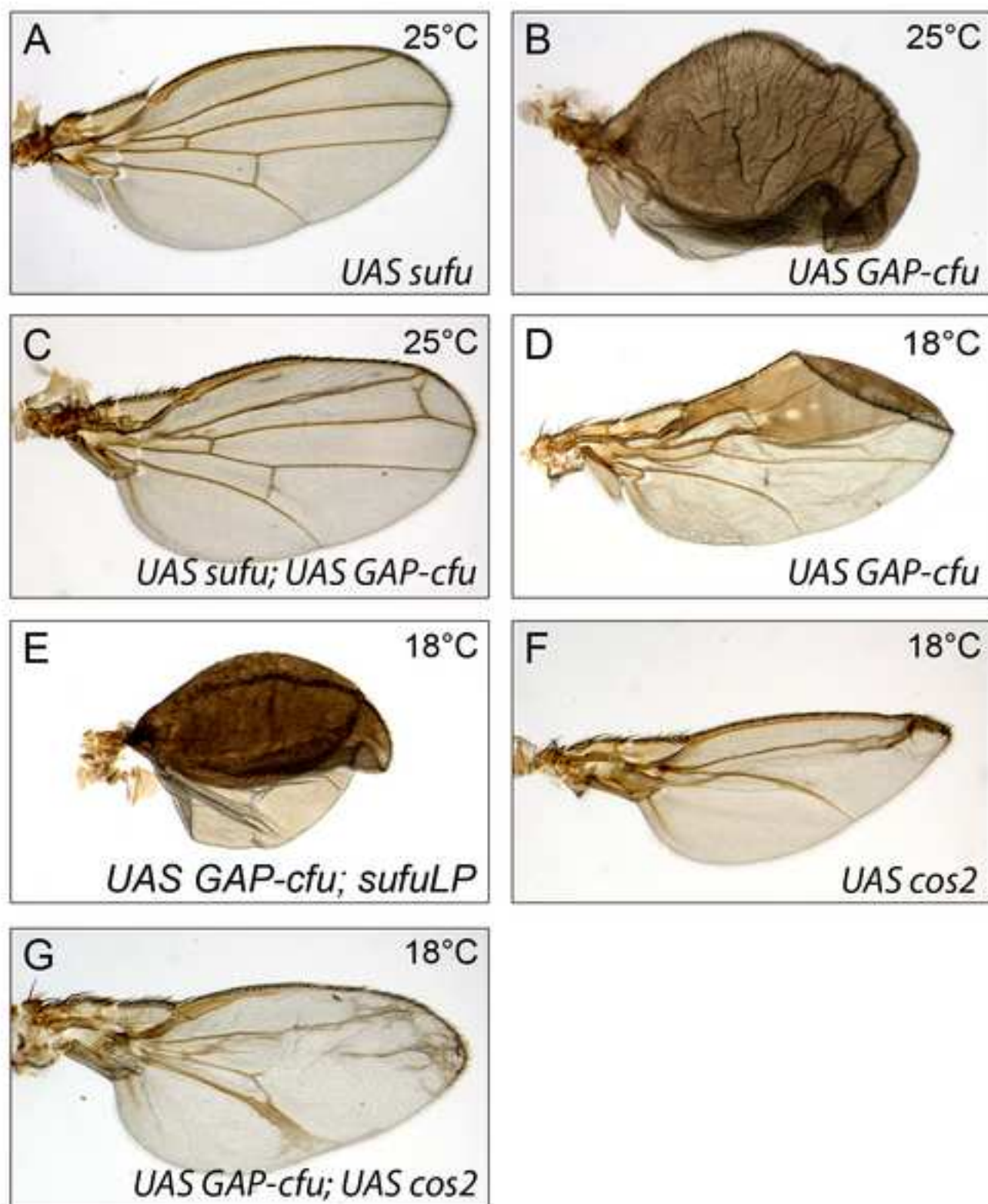
Supplemental bibliographie

1. Brand, A.H., Manoukian, A.S., and Perrimon, N. (1994). Ectopic expression in *Drosophila*. *Methods Cell Biol* 44, 635-654.
2. Rudolph, M.J., Amodeo, G.A., Bai, Y., and Tong, L. (2005). Crystal structure of the protein kinase domain of yeast AMP-activated protein kinase Snf1. *Biochem Biophys Res Commun* 337, 1224-1228.
3. Ascano, M., Jr., Nybakken, K.E., Sosinski, J., Stegman, M.A., and Robbins, D.J. (2002). The carboxyl-terminal domain of the protein kinase fused can function as a dominant inhibitor of hedgehog signaling. *Mol Cell Biol* 22, 1555-1566.
4. Ascano, M., Jr., and Robbins, D.J. (2004). An intramolecular association between two domains of the protein kinase Fused is necessary for Hedgehog signaling. *Mol Cell Biol* 24, 10397-10405.
5. Monnier, V., Dussillol, F., Alves, G., Lamour, I.C., and Plessis, A. (1998). Suppressor of fused links fused and Cubitus interruptus on the hedgehog signalling pathway. *Curr Biol* 8, 583-586.
6. Pham, A., Therond, P., Alves, G., Tournier, F.B., Busson, D., Lamour Isnard, C., Bouchon, B.L., Pr  at, T., and Tricoire, H. (1995). The Suppressor of fused gene encodes a novel PEST protein involved in *Drosophila* segment polarity establishment. *Genetics* 140, 587-598.
7. Ho, K.S., Suyama, K., Fish, M., and Scott, M.P. (2005). Differential regulation of Hedgehog target gene transcription by Costal2 and Suppressor of Fused. *Development* 132, 1401-1412.

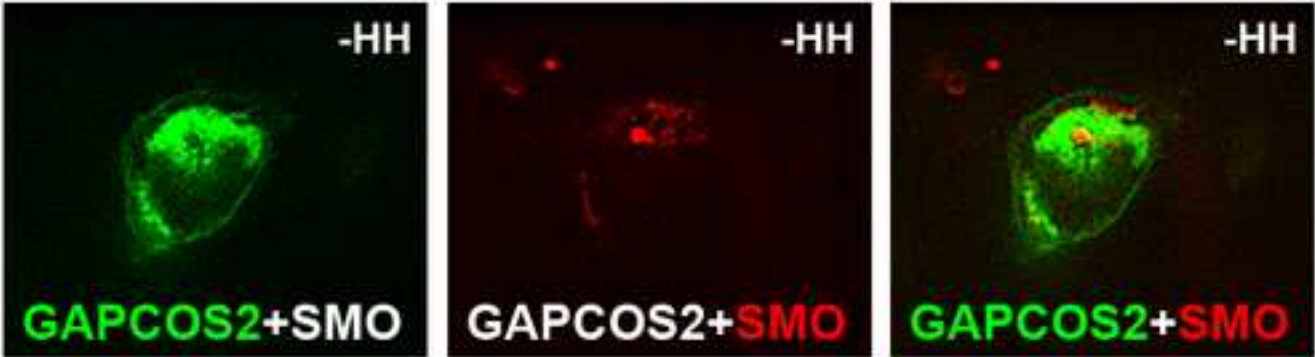
8. Dussillol-Godar, F., Brissard-Zahraoui, J., Limbourg-Bouchon, B., Boucher, D., Fouix, S., Lamour-Isnard, C., Plessis, A., and Busson, D. (2006). Modulation of the Suppressor of fused protein regulates the Hedgehog signaling pathway in *Drosophila* embryo and imaginal discs. *Dev Biol*.
9. Malpel, S., Claret, S., Sanial, M., Brigui, A., Piolot, T., Daviet, L., Martin-Lannere, S., and Plessis, A. (2007). The last 59 amino acids of Smoothened cytoplasmic tail directly bind the protein kinase Fused and negatively regulate the Hedgehog pathway. *Dev Biol* 303, 121-133.
10. Zhu, A.J., Zheng, L., Suyama, K., and Scott, M.P. (2003). Altered localization of *Drosophila* Smoothened protein activates Hedgehog signal transduction. *Genes Dev* 17, 1240-1252.
11. Taipale, J., Cooper, M.K., Maiti, T., and Beachy, P.A. (2002). Patched acts catalytically to suppress the activity of Smoothened. *Nature* 418, 892-897.
12. Fukumoto, T., Watanabe-Fukunaga, R., Fujisawa, K., Nagata, S., and Fukunaga, R. (2001). The fused protein kinase regulates Hedgehog-stimulated transcriptional activation in *Drosophila* Schneider 2 cells. *J Biol Chem* 276, 38441-38448.
13. Lee, T., and Luo, L. (2001). Mosaic analysis with a repressible cell marker (MARCM) for *Drosophila* neural development. *Trends Neurosci* 24, 251-254.
14. Capdevila, J., and Guerrero, I. (1994). Targeted expression of the signaling molecule decapentaplegic induces pattern duplications and growth alterations in *Drosophila* wings. *Embo J* 13, 4459-4468.
15. Brand, A.H., and Perrimon, N. (1993). Targeted gene expression as a means of altering cell fates and generating dominant phenotypes. *Development* 118, 401-415.
16. Pignoni, F., and Zipursky, S.L. (1997). Induction of *Drosophila* eye development by decapentaplegic. *Development* 124, 271-278.
17. Therond, P.P., Knight, J.D., Kornberg, T.B., and Bishop, J.M. (1996). Phosphorylation of the fused protein kinase in response to signaling from hedgehog. *Proc Natl Acad Sci U S A* 93, 4224-4228.
18. van den Heuvel, M., and Ingham, P.W. (1996). smoothened encodes a receptor-like serpentin protein required for hedgehog signalling. *Nature* 382, 547-551.

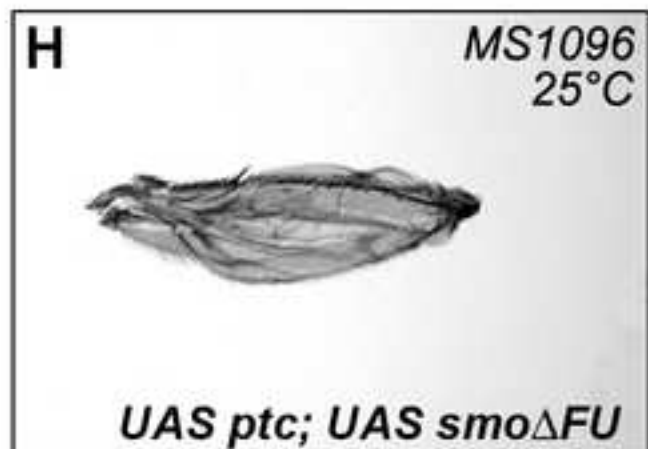
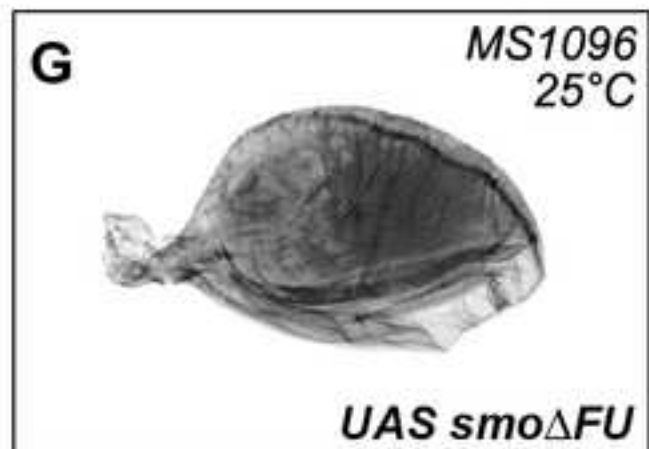
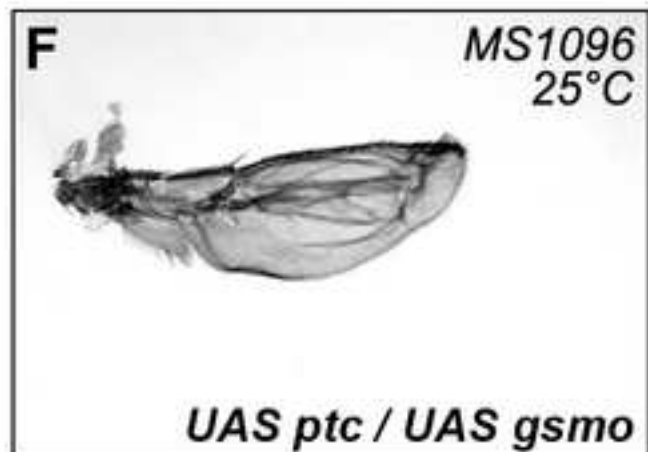
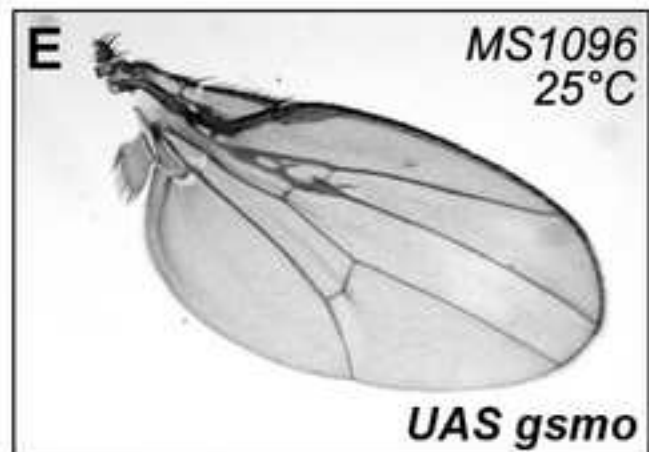
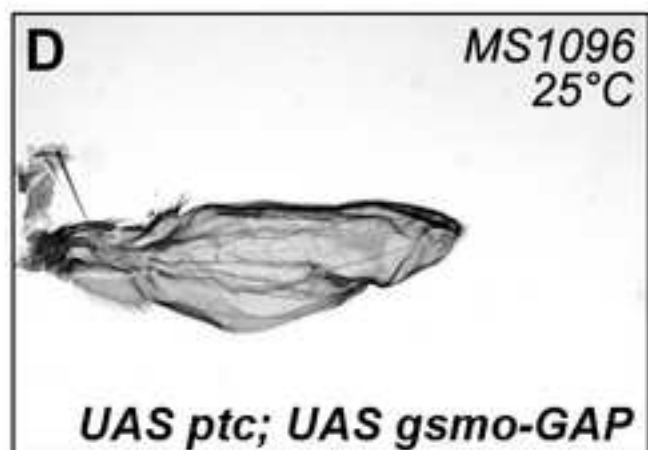
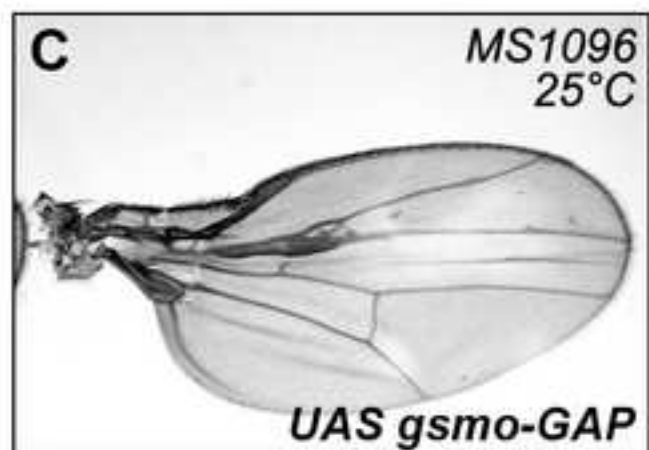
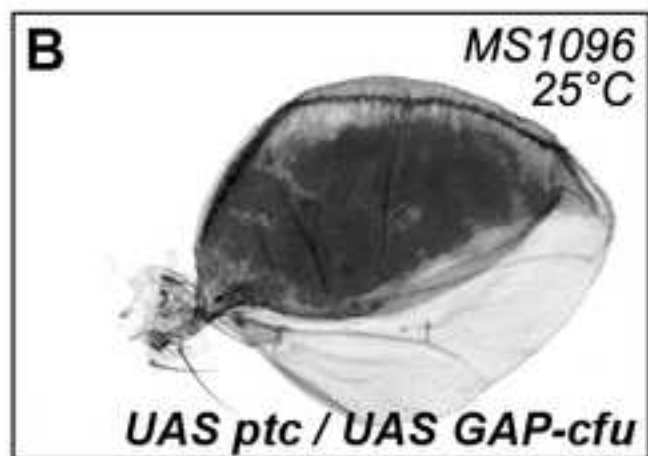
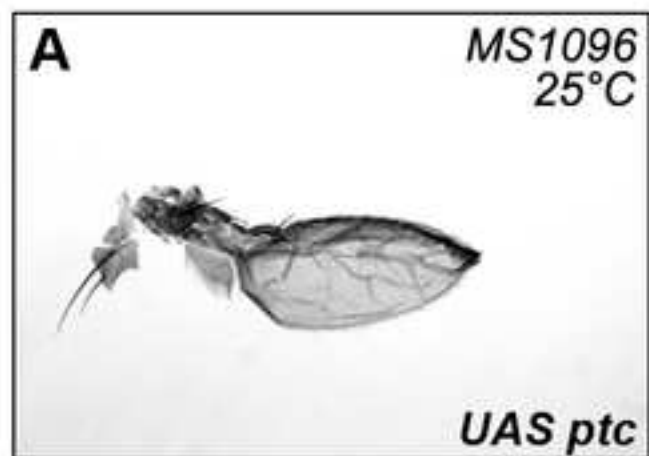




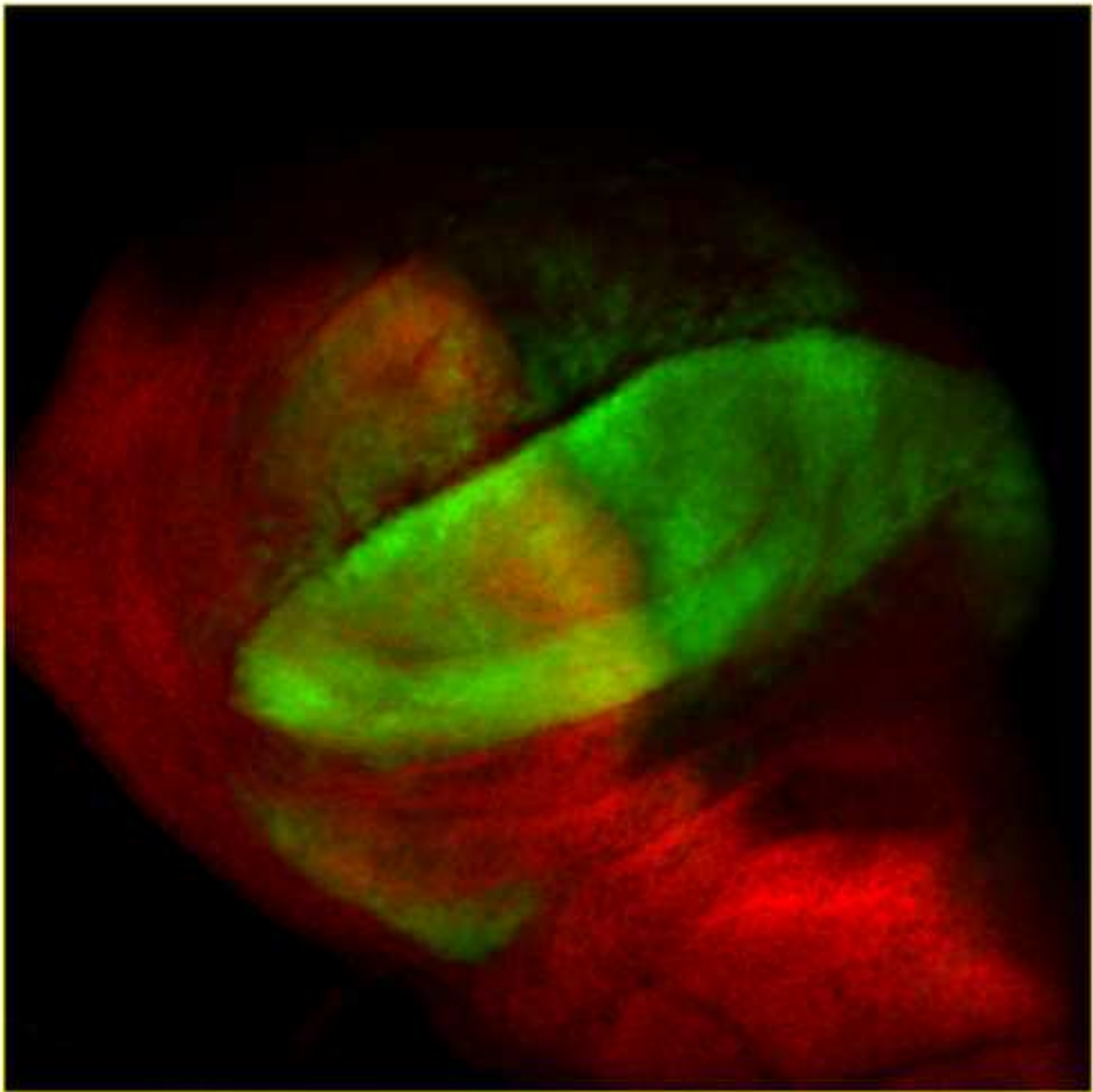


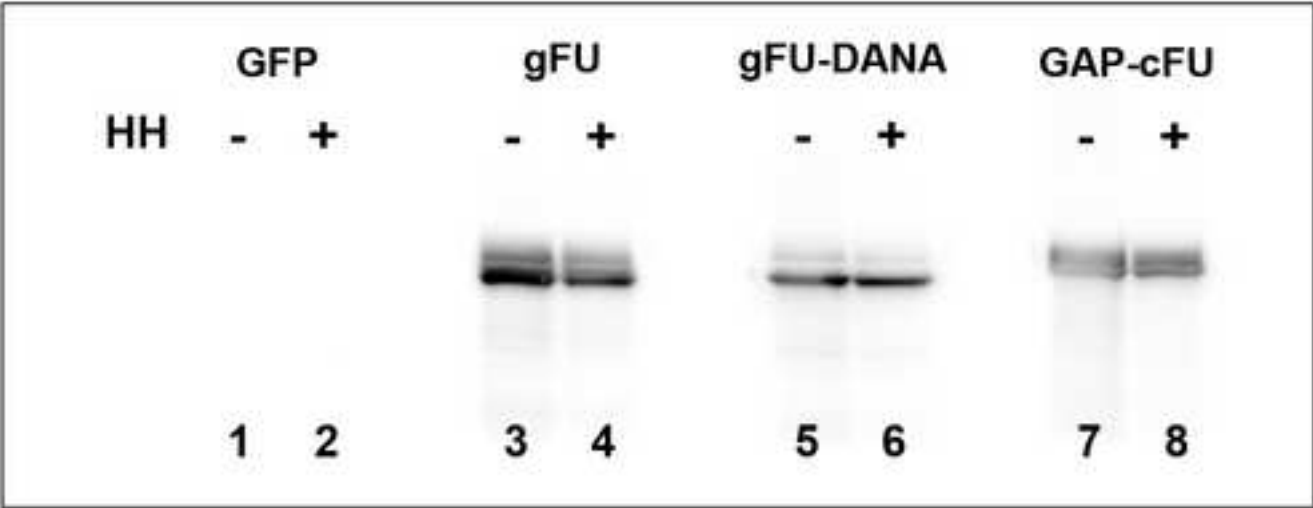
Supplemental figure 4

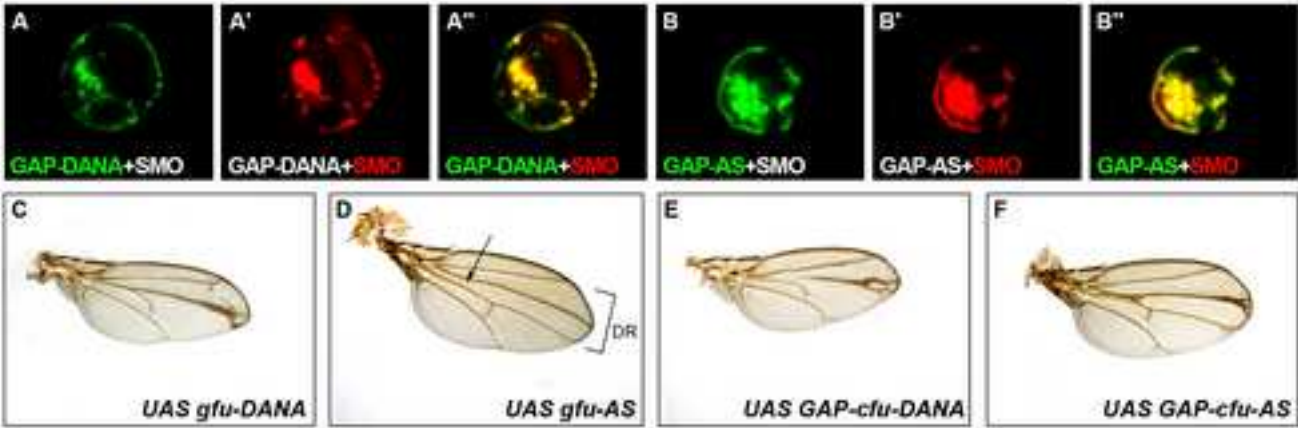


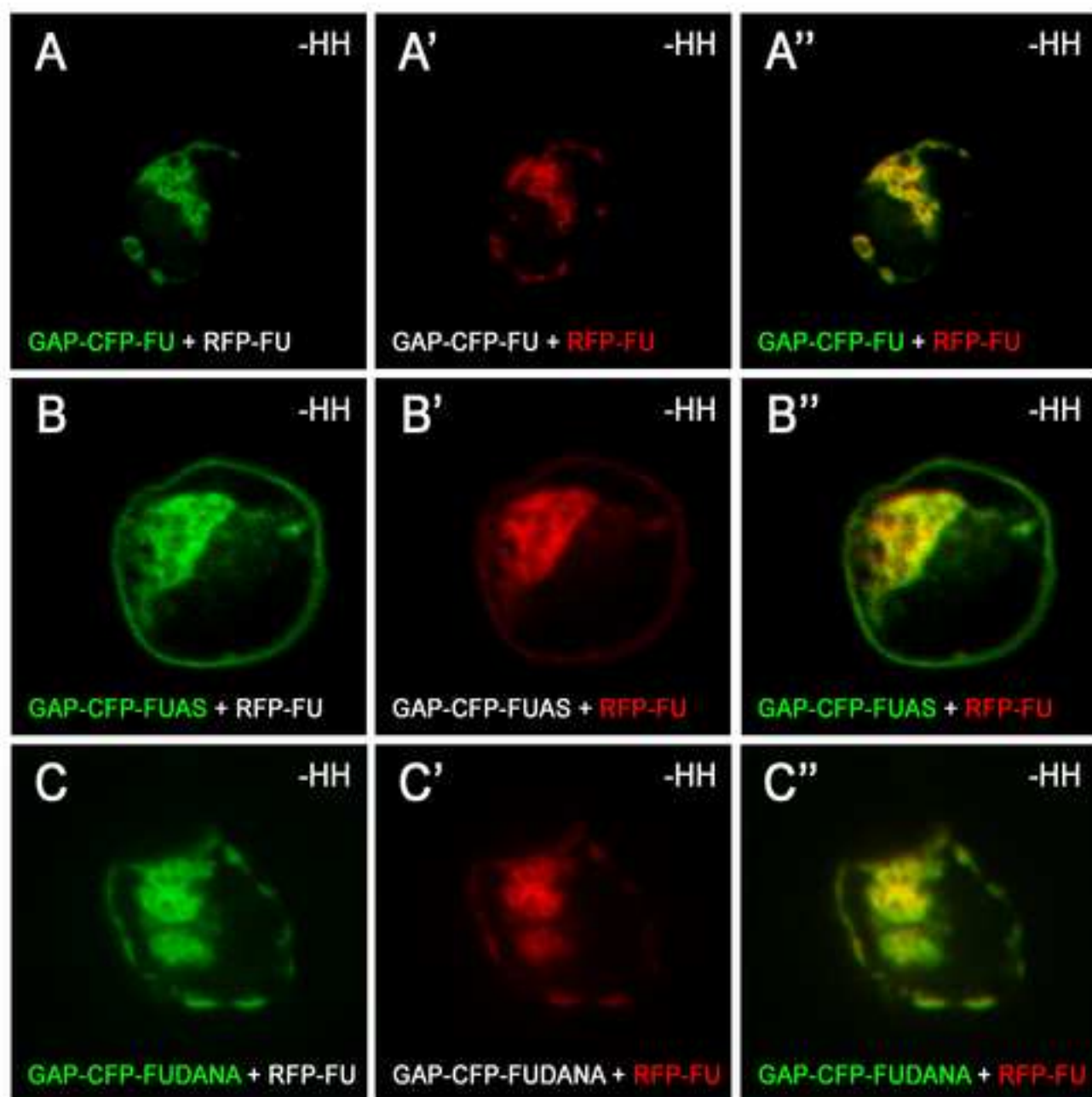


Supplemental figure 6









Supplemental Figure 10

